Electronic Supplementary Material (ESI) for Chemical Communications.

Supporting information

Imaging vicinal dithiol of arsenic-binding proteins in mouse brain with amplification by gold nanocluster $Au_{22}(GSH)_{18}$

Yin-Hao Li[#], Xing Wei[#], Xun Liu, Xiao-Ping Zhang, Yang Shu*, Jian-Hua Wang*

Research Center for Analytical Sciences, Department of Chemistry, College of Sciences, Northeastern University, Box 332, Shenyang 110819, China

*Corresponding Authors.

E-mail addresses: shuyang@mail.neu.edu.cn; jianhuajrz@mail.neu.edu.cn.

EXPERIMENTAL SECTION

Chemicals and Materials. Tetrachloroauric (Ⅲ) acid tetrahydrate ($HAuCl_4 \cdot xH_2O$), isopropyl alcohol (C_3H_8, 99.7%), hydrochloric acid (HCl), glycerol (99%), methanol (CH_3OH, 99.7%), ether ($C_4H_{10}O$, 99.5%) were obtained from Sinopharm Chemical Reagent Co., Ltd. (Shanghai, China). Glutathione (Reduced) (GSH, 98%), sodium hydroxide (NaOH, 96%), sodium borohydride ($NaBH_4$, 98%), acrylamide(AM, 99%), N,N′-methylenebis (acrylamide) (MBA, 99%), *p*-arsanilic acid (PASA, 98%), phenylhydrazine ($C_6H_5N_2H_3$), 1,2-ethanedithiol ($C_2H_6S_2$, 97%), N-(3-dimethylaminopropyl)-N′-ethylcarbodiimide hydrochloride (EDC, 98%), N-hydroxysuccinimide (NHS, 98%), N,N-dimethylformamide (DMF, 99.8%), DL-dithiothreitol (DTT, 98%) were purchased from Aladdin Reagent Co., Ltd. (Shanghai, China). Hemoglobin (Hb), concanavalin A (ConA), β-Casein (β-Cs), ovotransferrin (OTF), trypsin, myoglobin (Mb), lysozyme (LZ), glucose oxidase (GOD), ovalbumin (OVA), cytochrome c (cyt-c), transferrin (THR), bovine serum albumin (BSA), human serum albumin (HSA) were received from Sigma-Aldrich (St. Louis, MO, USA). All the reagents were of analytical reagent grade and used without further purification.

Instrumentation. UV-vis absorption spectra were measured with a UH5300 spectrophotometer (Hitachi, Japan) with a 1.0 cm quartz cell. Photoluminescence (PL) spectra were recorded on an F-7000 fluorescence spectrophotometer (Hitachi Ltd.,Tokyo, Japan). The size and morphology of the APE were observed on a JEM-ARM 200F transmission electron microscope (JEOL, Japan) using an accelerating voltage of 200 kV. An Agilent 6540 UHD Accurate-Mass Q-TOF LC/MS (Agilent Technologies, USA) equipped with an orthogonal ESI source was applied in the negative ionization mode for the identification of the gold nanoclusters. The samples were prepared in ultrapure water at a concentration of 10 mg/mL and directly injected 20 μL sample into the chamber for measurement. A triple-quadrupole inductively coupled plasma mass spectrometer (Agilent 8900, Agilent Technologies, CA, USA) were used for the quantification of gold and arsenic by measuring the isotope of ^{197}Au and ^{75}As. An NWR image laser ablation system (ESI, USA) was used in this work. This instrument equips with a 266 nm Nd: YAG laser. The LA system was coupled to a triple quadrupole ICP-MS (PerkinElmer, NexION 2000D, USA) for the analysis of

isotope of ^{197}Au and ^{75}As. Fourier transform infrared spectra (FT-IR) are recorded on a VERTEX 70 FT-IR spectrophotometer (Brooker, Germany) from 4000 to 400cm^{-1}.

Preparation of Au_{22} nanoclusters. Glutathione decorated gold nanoclusters $Au_{22}(GSH)_{18}$ were prepared according to previous approaches with reduction by $NaBH_4$. [1-3] $HAuCl_4$ (12.5 mL, 20 mM) and GSH (7.5 mL, 50 mM) were added to 200 mL ultrapure water. GSH not only serves as the ligand for the preparation of $Au_{22}(GSH)_{18}$, but also acts as a stabilizing agent. After rapid stirring for 5 min, the reaction medium was adjusted to pH 12 with 1.0 M NaOH solution. 100 μL of $NaBH_4$ solution (0.1 M) was then added with stirring at 800 rpm. The reaction mixture slowly changed from colorless to orange, and further turned to orange red after 0.5 h. It was then adjusted to pH 2.5 with 1.0 M HCl, and turned to dark-red. The reaction medium was stirred at 200 rpm under airtight conditions for 8 h, followed by concentration to ca. 20 mL by distillation under reduced pressure. 40 mL of isopropanol was then added, and the deep red precipitate was collected by centrifugation at 15000 rpm for 10 min. $Au_{22}(GSH)_{18}$ nanoclusters were finally dispersed in a 12% glycerol aqueous solution to 8 mg/mL, and subjected to polyacrylamide gel electrophoresis (PAGE, 30 wt% monomer) to separate and collect $Au_{22}(GSH)_{18}$.

Preparation of PAO-EDT. *P*-arsanilic acid (PASA, 10.85 g, 50 mmol) was dissolved in anhydrous methanol (60 mL), and the solution was heated under reflux. Thereafter, phenylhydrazine (10.3 mL, 100 mmol) was added dropwisely in 10 min, accompanying by production of N_2. The mixture was stirred for 1 h, and then the solvent was evaporated under reduced pressure. 85 mL water (85℃) and 60 mL NaOH solution (0.1 M) were added, followed by washing with ether (150 mL). After removing the ether phase, 40 mL of NH_4Cl solution (5 M) was added and the mixture was kept at 0℃ for 1 h to produce white precipitate of PAO. The precipitate was filtered through a Buchner funnel, followed by washing with 50 mL of ice water. The product was freeze-dried at −60℃ for 12 h under vacuum.

PAO (1.29 g, 6.42 mmol) was dissolved in 10 mL of absolute ethanol, and EDT (0.65 mL, 8.46 mmol) was added dropwisely under reflux. The reaction mixture was then stirred and refluxed for 30 min. The excess supernatant was removed after the reaction mixture was chilled in ethanol/ice. The PAO-EDT precipitate was recrystallized with 10 mL of ethanol, which was then filtered through a Buchner funnel, followed by washing with 10 mL of ice water. The product was freeze-dried at

−60℃ for 12 h under vacuum.

Preparation of Au_{22}-PAO-EDT (APE). $Au_{22}(GSH)_{18}$ (10 mg) was suspended in 2 mL ultrapure water. EDC (7.2 mg, EDC/$Au_{22}(GSH)_{18}$=36) and NHS (4.3 mg, NHS/EDC=1) were afterwards added and stirred for 30 min. Thereafter, PAO-EDT (2.36 mg, PAO-EDT/$Au_{22}(GSH)_{18}$=9) dissolved in 2 mL DMF was introduced and continuously stirred at room temperature for 16 h. 3000 Da ultrafiltration centrifuge tube (Merck Millipore, Germany) was finally used to remove the unreacted small molecules, and Au_{22}-PAO-EDT (APE) was obtained for future use.

Gold gelatin sections for LA-ICP-MS analysis. ^{197}Au standard solution was used to obtain a final concentration of 0-80 μg/g 15% gelatin (w/w) for quantitative analysis of ^{197}Au in matching mouse brain sections. The gelatin and Au standard solutions were mixed under stirring and heating at 60℃. The liquid Au-gelatin was transferred to the mold and cooled to a solid. The Au-gelatin standard was frozen in a cryostat at -20°C, then cut into sections with a thickness of 10 μm. The sections were then mounted on a microscope slide and dried naturally at room temperature for 24 h. The gold gelatin sections were stored in -20 ℃ for future use.

Preparation of mouse brain section. Kunming mice (female, 20-22g) were used as model for the present study. All the animal experiments were carried out in accordance with current guidelines for the care of laboratory animals and were approved by Animal and Medical Ethics Committee of Northeastern University. The mice were housed in a controlled light (12-hour light/dark cycle), temperature and humidity conditions with free access to food and water. The animals were divided into three groups, i.e., control group, low-arsenic group and high-arsenic group. The drinking water contains 0, 4, 400 mg/L of sodium arsenite for the three groups for facilitating free drinking experiment. The mice were sacrificed after three weeks of breeding. After the mice were anesthetized, they were perfused with 4% paraformaldehyde to remove the blood in the brain tissue. Then the brain was soaked in 4% paraformaldehyde for 24 h, followed by further soaking in 15% and 30% sucrose solutions for 24 h. Before sectioning, the mouse brain was rinsed with DI water and infiltrate through optimal cutting temperature compound (OCT), and then sectioned by cryostat with a thickness of 10 μm.

Immunohistochemistry of the mouse brain section with APE. The mouse

brain sections were taken out and washed three times with 10 mM Tris-HCl buffer (pH 8.0), each for 10 min. Then the sections were incubated with 0.1% Triton X-100 in 10 mM Tris-HCl buffer (pH 8.0) for 20 min. The above washing procedure was repeated to remove Triton X-100. 1 mg/ml Dithiothreitol (DTT) was used to process the sections overnight. Continue the washing step to remove the excess DTT. APE (10 μg/mL) were added and incubated overnight at 4℃, followed by washing with 10 mM Tris-HCl buffer. After dried naturally at room temperature for 24 h, the mouse brain sections were stored in -20℃ for future use.

Polyacrylamide gel electrophoresis (PAGE). PAGE separation of the AuNCs species. The separation of AuNCs species was processed on a DYCZ-24F (BEIJING LIUYI) system. The total contents of the acrylamide monomers (19:1= monomer: crosslinker) were 30 wt% and 4 wt% for the resolving and stacking gels, respectively. The electrophoresis buffer was made of 192 mM glycine and 25 mM tris (hydroxymethyl) aminomethane. 50 μL sample solutions (8 mg/mL crude AuNCs in 12 vol% glycerol aqueous solution) were loaded into the wells of the stacking gel. The electrophoresis was allowed to run for ~10 h at a constant voltage of 280 V by circulating condensate to cool down at room temperature. After the electrophoresis is complete, the top orange AuNCs band was cut and divided them into small pieces and soak them in ultrapure water overnight to diffuse the gold nanocluster $Au_{22}(GSH)_{18}$. The resulting solutions were filtered by use of a filter with 0.22 μm pore size, and 3000 Da ultrafiltration centrifuge tube was used to remove excess impurities.

PAGE separation of protein and APE. The separation of protein and APE was processed on a DYCZ-24F (BEIJING LIUYI) system. The total contents of the acrylamide monomers (19:1= monomer: crosslinker) were 15 wt% and 4 wt% for the resolving and stacking gels, respectively. Samples were labeled in Tris-HCl buffer (pH 8.0) with a final concentration of protein at 1.25 mg/ml, APE or Au_{22} at 2.5 mg/ml for 1 h. After labeling, the samples were mixed with 1/4 sample volume of 5×loading buffer, 20 μL sample solutions were loaded into the wells of the stacking gel. The electrophoresis was allowed to run for ~5 h at a constant voltage of 200 V by circulating condensate to cool down at room temperature. In electrophoresis, due to the large difference in the m/z between APE and protein, they can be well separated. After the electrophoresis was complete, the protein bands were cut for microwave digestion, diluted to an appropriate concentration for ICP-MS detection.

The preparation of arsenic-binding proteins. Due to the high activity of the arsenic-binding proteins, it is difficult to be stored in a reduced state for a long time. Therefore, the protein needs to be reduced before each use. For this purpose, the proteins (10^{-4} mM for BSA, HSA, THR) with DTT (50 mM) were mixed and reduced at 4 °C for 12 h. The excess DTT were removed through a 10 KDa cut off desalting column.

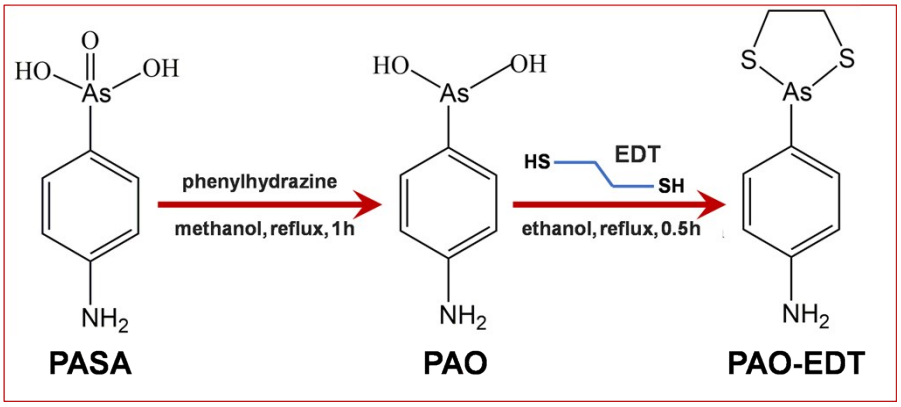

Figure S1. Chemical path for the preparation of PAO-EDT.

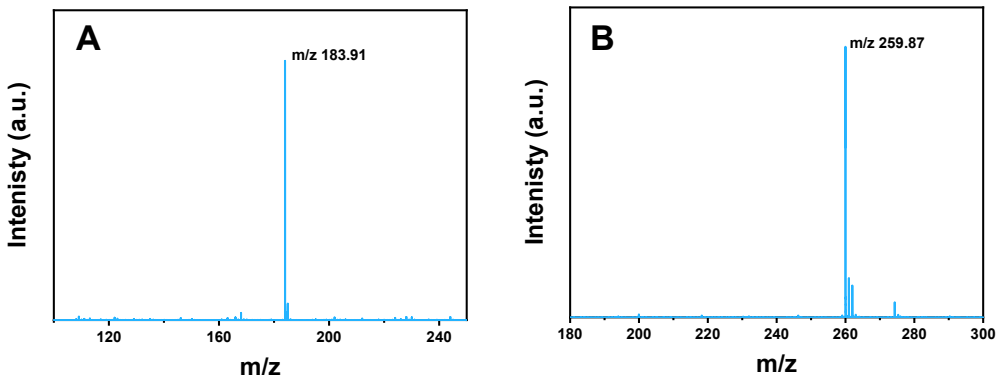

Figure S2. ESI mass spectra of PAO (A) and PAO-EDT (B).

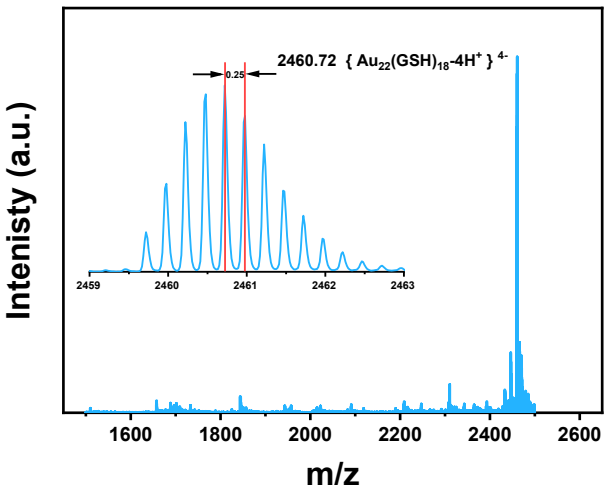

Figure S3. ESI mass spectra of the gold nanocluster $Au_{22}(GSH)_{18}$, the inset is the isotope pattern of $Au_{22}(GSH)_{18}$.

The purified AuNCs were collected and analyzed by ESI-MS in negative-ion mode. It illustrated a group of intense peaks at m/z ~2460.72, with the distance of 0.25 between two adjacent peaks. It indicates that the ionized AuNCs carry four units of negative charge, so the molecular weight of AuNCs is 9842.88 Da, which is extremely close to the theoretical molecular weight of $Au_{22}(GSH)_{18}$ of 9841.60 Da.

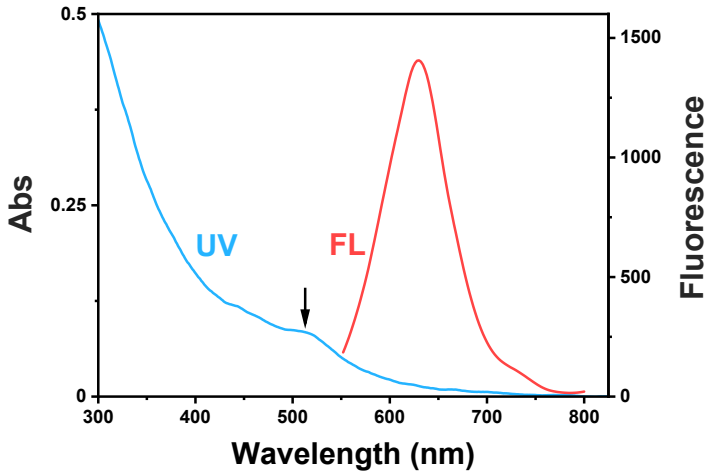

Figure S4. UV-vis absorption spectra (blue) and fluorescence spectra with an excitation wavelength at λ_{ex}=520 nm (red) for 1.0 mg/mL $Au_{22}(GSH)_{18}$ nanocluster suspended in aqueous medium.

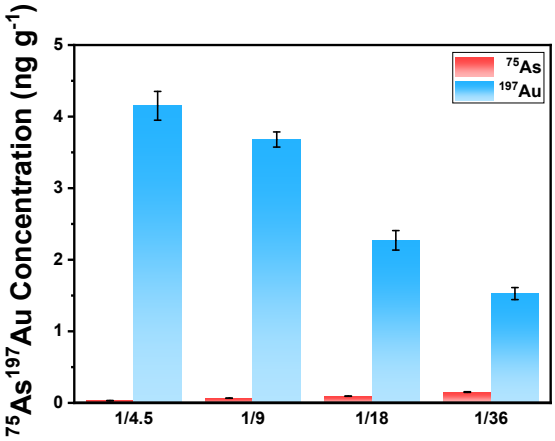

Figure S5. The content of ^{197}Au and ^{75}As in the four APEs derived by ICP-MS. The abscissa indicates the ratio of $Au_{22}(GSH)_{18}$ to PAO-EDT in the amidation reaction.

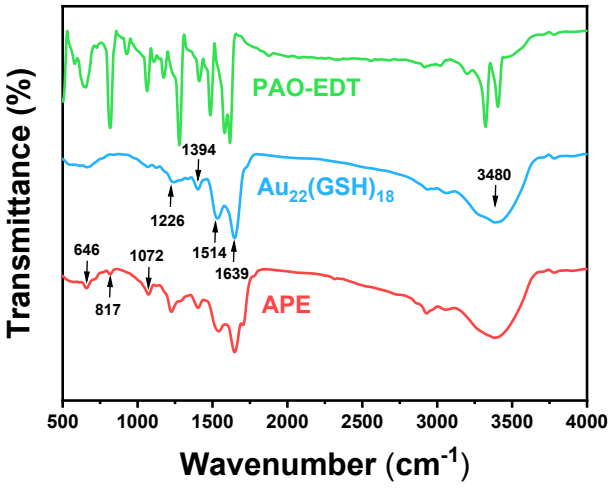

Figure S6. FT-IR spectrum of PAO-EDT, $Au_{22}(GSH)_{18}$ and APE.

FT-IR spectra indicated that both $Au_{22}(GSH)_{18}$ and APE ($Au_{22}(GSH)_{18}$: PAO-EDT=1: 9) exhibit a strong absorption band at 3480 cm^{-1}, which may be attributed to the combination of O-H and N-H stretching vibrations in GSH. The absorptions at 1639 cm^{-1}, 1514 cm^{-1}, and 1226 cm^{-1} correspond to the amide groups I, II, and III, respectively, are ascribed to the stretching vibrations of C=O, N-H and C-N.[4] Due to the wagging and twisting vibrations of the $-CH_2$ group, an obvious absorption is identified at 1394 cm^{-1}. After PAO-EDT is modified to $Au_{22}(GSH)_{18}$, the three characteristic absorption bands for PAO-EDT, i.e., 1072 cm^{-1}, 817 cm^{-1}, and 646 cm^{-1} were observed for APE with respect to those encountered in $Au_{22}(GSH)_{18}$. The absorptions at 1072 and 817 cm^{-1} are due to the in-plane and out-of-plane C-H bending vibrations for the benzene ring, respectively. The absorption at 646 cm^{-1} was caused by As-C telescopic vibration.[5]

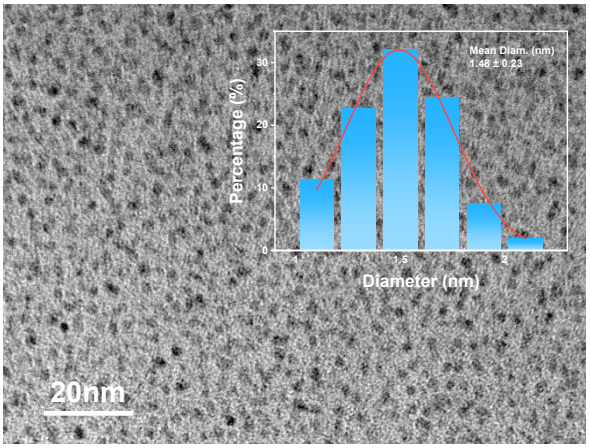

Figure S7. TEM images of the prepared APEs, the inset is the size/diameter distribution of the APEs.

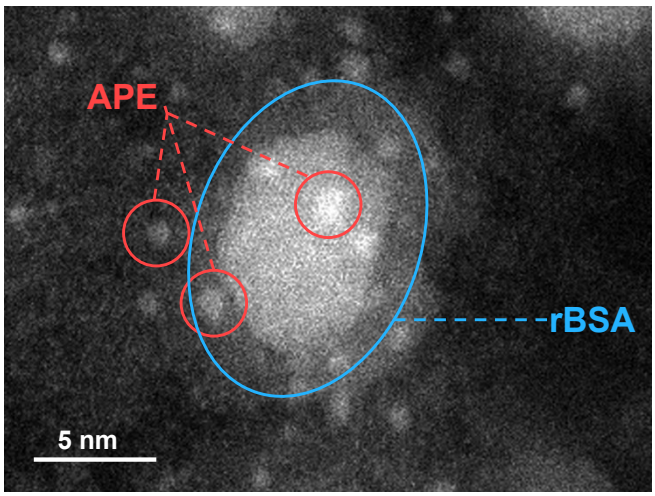

Figure S8. Scanning transmission electron microscopy (STEM) image for the illustration of assembly of APE onto the surface of rBSA to form APE@rBSA composite.

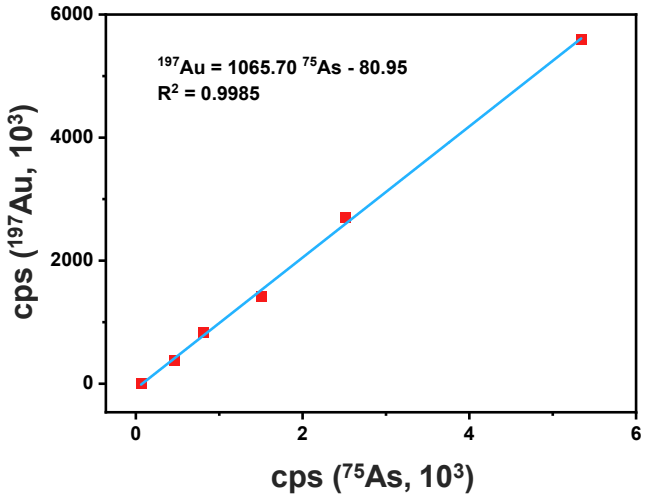

Figure S9. The correlation of ^{197}Au and ^{75}As response in ICP-MS detection (counts per second, cps) in APE ($Au_{22}(GSH)_{18}$: PAO-EDT=1: 9).

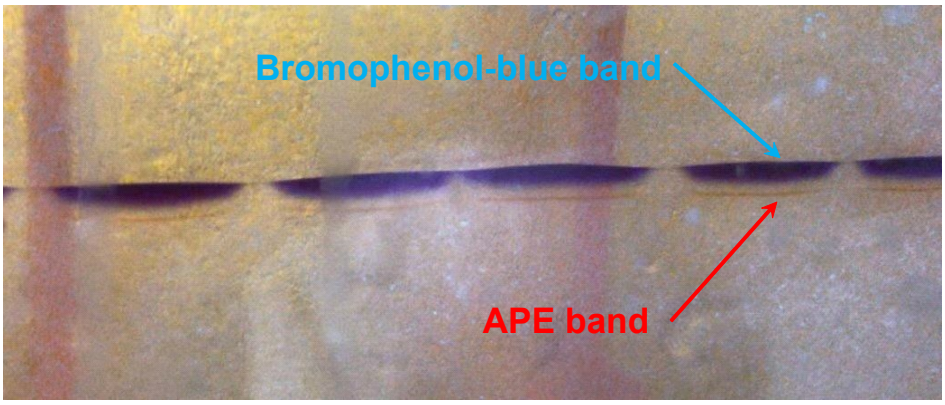

Figure S10. Schematic illustration for the separation of protein and APE by PAGE.

The migration rate of most proteins in PAGE is slower than bromophenol-blue, the protein band should be observed above the bromophenol-blue band, thus bromophenol-blue maybe used to judge the progress of PAGE as indicator. In Figure S10, APE band is below the bromophenol-blue band during the PAGE process, this indicated that the migration of APE is faster than bromophenol-blue. Considering the fact that migration rate of protein is slower than that of bromophenol-blue in PAGE, the migration of APE is faster than the proteins, which proves that the mixture of protein and APE may be separated by PAGE.

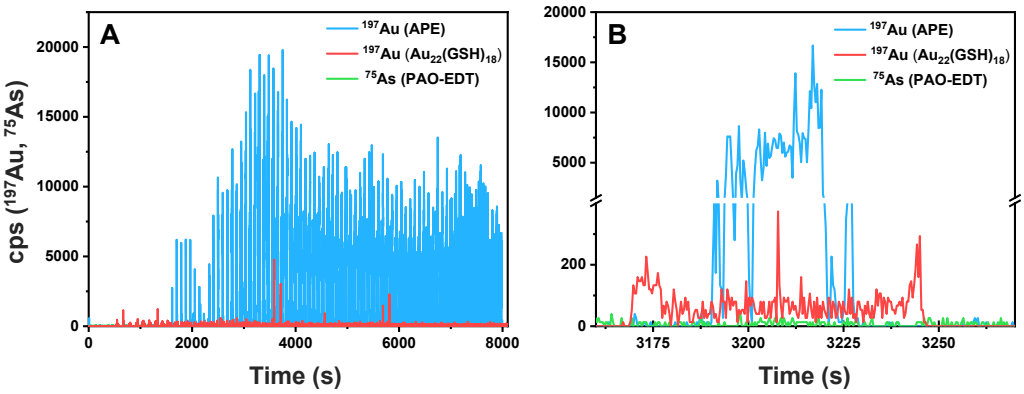

Figure S11. (A) Detection of ^{197}Au (labeled by APE and $Au_{22}(GSH)_{18}$) and ^{75}As (labeled by PAO-EDT) in the mouse brain under time-resolved scans by LA-ICP-MS. (B) The close-up illustration in Figure A.

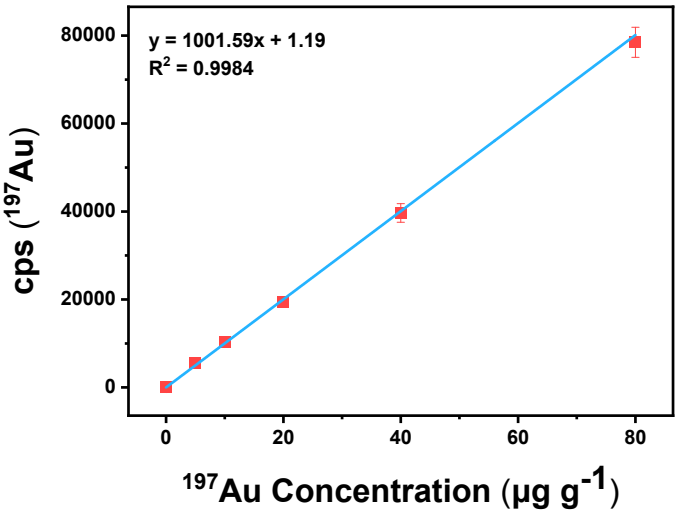

Figure S12. Calibration curve obtained for ^{197}Au by LA-ICP-MS using matrix matched standard of gelatin.

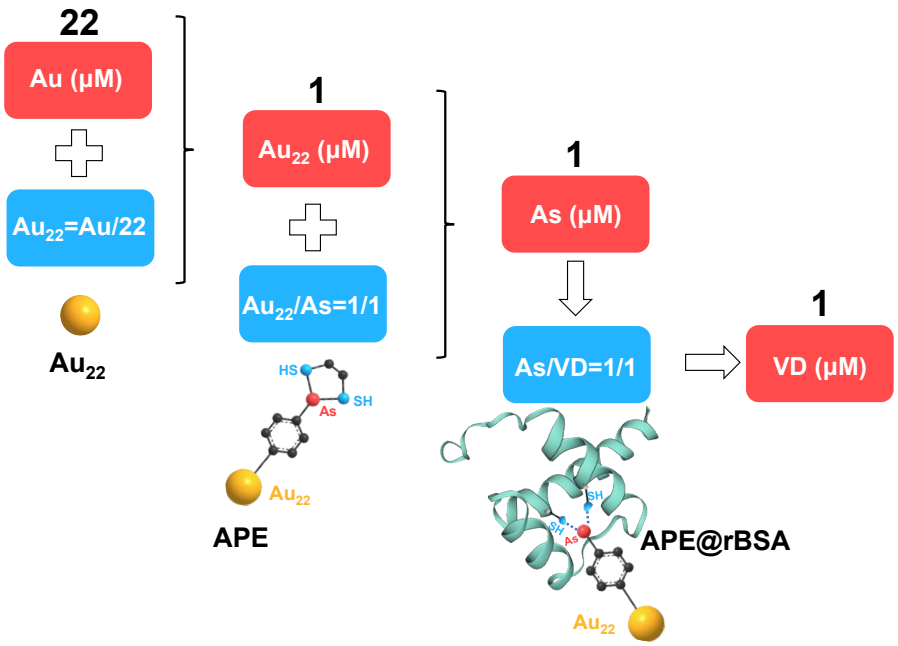

Figure S13. Schematic illustration for correlating the concentration of ^{197}Au derived by LA-ICP-MS to the content of VD in the mouse brain tissue section.

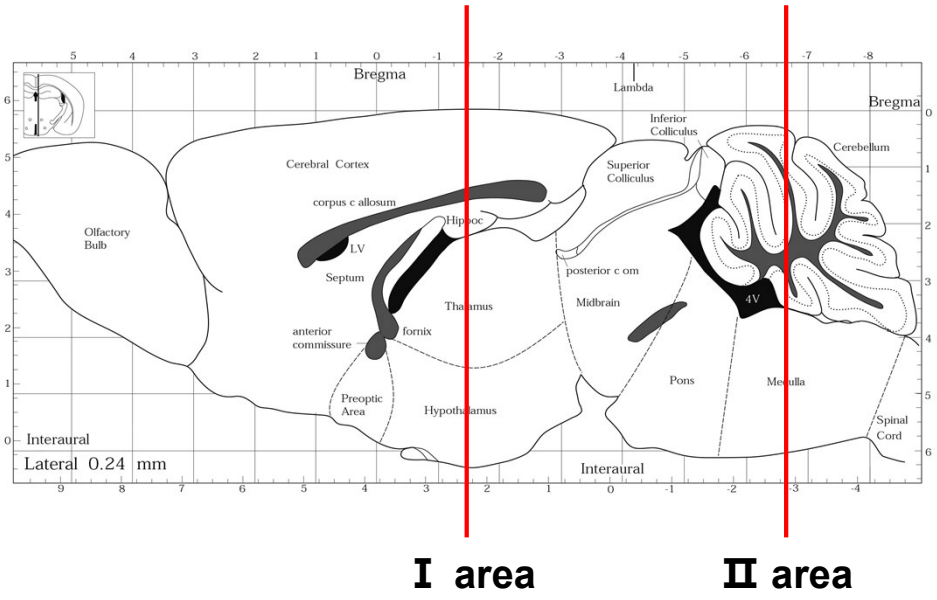

Figure S14. The cutting position map of mouse brain section.[6] Ⅰ area contains cerebral cortex, hippocampus, epithalamus and hypothalamus. Ⅱ area contains cerebellum and brain stem.

Table S1. Comparison of the limit of detection of the present protocol with some fluorescence approaches for the assay of rBSA.

Detection	Probe	LOD (nM)	Ref
Fluorescence	Naphthalimide-PAO-EDT	140	1
Fluorescence	Coumarin-PAO-BAL	140	2
Fluorescence	2-(4-dimethylaminophenyl)-4-(2-car-boxyphenyl)-7-diethylamino-1-benzopyrylium-PAO-EDT	15	3
Fluorescence	7-diethylamincoumarin-PAO-EDT	2.6	4
Fluorescence	Indolium-conjugated-Benzoxadiazole-PAO-EDT	2	5
Fluorescence	Merocyanine-Schiff-Base-PAO-EDT	15	6
Fluorescence	4-amino-1,8-naphthalimide-PAO-BAL	19	7
ICP-MS	$Au_{22}(GSH)_{18}$-PAO-EDT	0.6	This work

References

1. Huang, C.; Yin, Q.; Zhu, W.; Yang, Y.; Wang, X.; Qian, X.; Xu, Y., Highly Selective Fluorescent Probe for Vicinal-Dithiol-Containing Proteins and In Situ Imaging in Living Cells. *Angew. Chem., Int. Ed.* **2011**, *50*, 7551-7556.

2. Huang, C.; Jia, T.; Tang, M.; Yin, Q.; Zhu, W.; Zhang, C.; Yang, Y.; Jia, N.; Xu, Y.; Qian, X., Selective and ratiometric fluorescent trapping and quantification of protein vicinal dithiols and in situ dynamic tracing in living cells. *J. Am. Chem. Soc.* **2014**, *136*, 14237-14244.

3. Wang, Y.; Yang, X. F.; Zhong, Y.; Gong, X.; Li, Z.; Li, H., Development of a red fluorescent light-up probe for highly selective and sensitive detection of vicinal dithiol-containing proteins in living cells. *Chem. Sci.* **2016**, *7*, 518-524.

4. Wang, Y.; Zhong, Y.; Wang, Q.; Yang, X.-F.; Li, Z.; Li, H., Ratiometric Fluorescent Probe for Vicinal Dithiol-Containing Proteins in Living Cells Designed via Modulating the Intramolecular Charge Transfer–Twisted Intramolecular Charge Transfer Conversion Process. *Anal. Chem.* **2016,** *88*, 10237-10244.

5. Liu, F.; Liu, H. J.; Liu, X. J.; Chen, W.; Wang, F.; Yu, R. Q.; Jiang, J. H.,

Mitochondrion-Targeting, Environment-Sensitive Red Fluorescent Probe for Highly Sensitive Detection and Imaging of Vicinal Dithiol-Containing Proteins. *Anal. Chem.* **2017,** *89*, 11203-11207.

6. Zhang, S.; Chen, G.; Wang, Y.; Wang, Q.; Zhong, Y.; Yang, X. F.; Li, Z.; Li, H., Far-Red Fluorescent Probe for Imaging of Vicinal Dithiol-Containing Proteins in Living Cells Based on a pKa Shift Mechanism. *Anal. Chem.* **2018,** *90*, 2946-2953.

7. Hu, G.; Jia, H.; Hou, Y.; Han, X.; Gan, L.; Si, J.; Cho, D.-H.; Zhang, H.; Fang, J., Decrease of Protein Vicinal Dithiols in Parkinsonism Disclosed by a Monoarsenical Fluorescent Probe. *Anal. Chem.* **2020,** *92*, 4371-4378.

Table S2. The amount of VD in mouse brain sections. The mouse brain sections were incubated with PAO-EDT followed by microwave digestion and ICP-MS detection.

	VD amount (nmol)		VD amount (nmol)
1	1.70 ± 0.07	6	2.23 ± 0.11
2	1.81 ± 0.09	7	2.26 ± 0.09
3	1.89 ± 0.05	8	2.32 ± 0.12
4	2.04 ± 0.04	9	2.35 ± 0.04
5	2.10 ± 0.09	10	2.43 ± 0.06

Table S3. The operating parameters for ICP-MS detection.

Parameter	Setting
Radiofrequency power (W)	1550
Plasma Ar gas flow (L min^{-1})	15
Auxiliary Ar gas flow (L min^{-1})	1
Carrier Ar gas flow (L min^{-1})	0.99
Makeup Ar gas flow (L min^{-1})	0.11
KED flow (mL min^{-1})	7
Dwell time (ms)	100
Isotope monitored	^{75}As, ^{197}Au

Table S4. The operating parameters for LA-ICP-MS detection.

Laser ablation (ESI NWR imaging)	
Laser	Nd: YAG
Wavelength (nm)	266
Fluence (J cm^{-2})	2.5
Scan speed (μm s^{-1})	150
Repetition frequency (Hz)	50
Spot size (μm)	50
Distance between lines (μm)	50
He gas flow (L min^{-1})	0.7
Ablation mode	Line
ICP-MS (PerkinElmer, NexION 2000D)	
Nebulizer gas flow (L min^{-1})	1.18
Auxiliary gas flow (L min^{-1})	1.2
Plasma gas flow (L min^{-1})	15
KED flow (mL min^{-1})	7
RF Power (W)	1500
Analog stage voltage (W)	-1550
Dwell time (ms)	15
Sweeps	5
Scan mode	Peak hopping
Isotopes	^{75}As, ^{197}Au

REFERENCES

1. Yu, Y.; Luo, Z.; Chevrier, D. M.; Leong, D. T.; Zhang, P.; Jiang, D.-E.; Xie, J., Identification of a Highly Luminescent $Au_{22}(SG)_{18}$ Nanocluster. *J. Am. Chem. Soc.* **2014**, 136, 1246-1249.

2. Pyo, K.; Thanthirige, V. D.; Kwak, K.; Pandurangan, P.; Ramakrishna, G.; Lee, D., Ultrabright Luminescence from Gold Nanoclusters: Rigidifying the Au(I)-Thiolate Shell. *J. Am. Chem. Soc.* **2015**, 137, 8244-50.

3. Pyo, K.; Ly, N. H.; Han, S. M.; Hatshan, M. b.; Abuhagr, A.; Wiederrecht, G.; Joo, S.-W.; Ramakrishna, G.; Lee, D., Unique Energy Transfer in Fluorescein-Conjugated Au_{22} Nanoclusters Leading to 160-Fold pH-Contrasting Photoluminescence. *J. Phys. Chem. Lett.* **2018**, 9, 5303-5310.

4. Hu, C.; Yang, D.-P.; Xu, K.; Cao, H.; Wu, B.; Cui, D.; Jia, N., Ag@BSA Core/Shell Microspheres As an Electrochemical Interface for Sensitive Detection of Urinary Retinal-Binding Protein. *Anal. Chem.* **2012**, *84*, 10324-10331.

5. Xu, S.; Sabino, F. P.; Janotti, A.; Chase, D. B.; Sparks, D. L.; Rabolt, J. F., Unique Surface Enhanced Raman Scattering Substrate for the Study of Arsenic Speciation and Detection. *J. Phys. Chem. A* **2018**, *122*, 9474-9482.

6. Konsman, J.-P., The mouse brain in stereotaxic coordinates: Second Edition (Deluxe) By Paxinos G. and Franklin, K.B.J., Academic Press, New York, 2001, ISBN 0-12-547637-X. *Psychoneuroendocrinology* **2003,** *28* , 827-828.